

ground-state cis-keto forms. Our kinetic data do imply, however, that there must be a strong variation in radiationless transition rate with angle in the excited state of HBT.

In various frozen environments at 4 K, this large angle torsional motion is negligible on the time scale of the  $^1\pi-\pi^*$  excited state fluorescence. Nevertheless, one might envision a small amplitude  $C_1-C_7$  torsional relaxation into some sort of local minimum on the potential-energy surface. It is known, for example, that some torsional relaxation occurs in the excited state of biphenyl isolated in solid neon and argon at 4.2 K.<sup>2</sup> In this regard it is useful to compare our SA and HBT data for the  $A \rightarrow B$  transient. As previously discussed, the data are remarkably similar with only small spectral shifts and changes in rates. Theoretically we might expect the torsional potential energy surfaces and moments of inertia to be different in the two cases, as SA has three, presumably coupled, torsional motions while HBT has only one well-defined torsion of  $C_1-C_7$ . The similarity of the HBT and SA results, and the very weak "viscosity" dependence for HBT observed in Table I, seems to support the idea that torsional relaxation does not principally influence the  $A \rightarrow B$  transient behavior at 4 K.

Very recently we have observed that similar blue-shifted transients occur on the  $\approx 10$ -ps time scale in the lowest  $^1\pi-\pi^*$  excited states of anthracene and tetracene in 4 K frozen solutions.<sup>11</sup> Like SA and HBT, these molecules have relaxed fluorescence spectra with relatively sharp blue edges. Unlike SA and HBT, however, excited-state anthracene and tetracene are planar aro-

matic compounds without known torsional normal modes. In these latter two molecules, we conclude that we have directly time resolved the excited state vibrational energy redistribution and/or relaxation into the environment.

In view of these arguments, we feel that the  $A \rightarrow B$  transient behavior in both HBT and SA appears to represent a direct measure of excited state vibrational energy redistribution and/or relaxation. As previously mentioned, the nascent cis-keto tautomer produced by proton transfer probably has appreciable excess vibrational energy in the bonds involved in the tautomerism. Unfortunately, there are no quantitative structural or thermodynamic data on the relative stability of the keto and enol tautomers. This initial distribution will evolve intramolecularly and ultimately relax into the local environment, as a function of time. These processes will affect the emission spectrum, and it may be that our ability to readily detect them in SA and HBT is related to the unusually sharp emission spectra (Figure 1).

These results, which should also be examined in molecules having better spectral resolution and firm excited state vibrational assignments, may have general implications in the field of picosecond molecular dynamics. In many important biological and chemical systems, the electronic spectra are so broad as to preclude any clear measurement of vibrational excitation based upon the shape of the electronic spectra. If a chemical reaction, isomerization, or electron or proton transfer occurs in an excited state, one does not normally know whether the process occurs from a vibrationally relaxed or "hot" initial state. We now have the first data which suggest that relaxation in large organic species occurs on the  $\sim 10$ -ps scale in low-temperature aprotic solutions.<sup>11</sup> It is possible therefore that some processes which have time constants much faster than  $\sim 10$  ps might initially proceed from a vibrationally "hot" electronic state.

(11) P. F. Barbara, P. M. Rentzepis, and L. E. Brus, *J. Chem. Phys.*, in press.

(12) After submission of this manuscript, an interesting and rather indirect measurement of room temperature vibrational thermalization has been reported: K. J. Choi and M. R. Topp, *Chem. Phys. Lett.*, **69**, 441 (1980).

## Ethylenediamine and Aminoacetonitrile Catalyzed Decarboxylation of Oxalacetate

Daniel L. Leussing\* and N. V. Raghavan

Contribution from the Chemistry Department, The Ohio State University, Columbus, Ohio 43210. Received December 18, 1979

**Abstract:** Monoprotonated ethylenediamine ( $\text{ENH}^+$ ) and aminoacetonitrile (AAN) are highly effective catalysts for the decarboxylation of oxalacetate ( $\text{OA}^{2-}$ ) with the latter amine showing 50% faster rates. The mechanisms of the reactions are the same as that earlier proposed by Guthrie and Jordan<sup>4</sup> from studies on the decarboxylation of acetoacetate ( $\text{AA}^-$ ): amine and keto acid react to form ketimine which either decarboxylates or is competitively converted to enamine. We find that a proton is required to effect decarboxylation, but it also promotes enamine formation, the more so the greater basicity of the parent amine. Owing to this side reaction, the more basic amines tend to show lower catalytic activity with respect to decarboxylation. A second effect also contributes to the high activity of AAN: even though the rate constants for imine formation appear to be roughly similar with AAN and  $\text{ENH}^+$ , proton catalysis has a much larger net influence on the AAN rate because changes in  $[\text{H}^+]$  are not canceled by inverse changes in [amine]. 4-Ethylloxalacetate forms an adduct with  $\text{ENH}^+$  that has a considerably greater enamine content and a higher stability than its  $\text{OA}^{2-}$  analogue. These differences in substrate behavior must be taken into account when esters are used as models for the parent keto acids in these reactions. Comparison of our results with those previously published for  $\text{OA}^{2-}$  decarboxylation catalyzed by a partially quaternized poly(ethylenimine) suggests that  $\text{OA}^{2-}$  is predominantly bound to the quaternary amine sites but decarboxylation likely proceeds via a Schiff-base mechanism.

Amine-catalyzed decarboxylation of  $\beta$ -keto acids has aroused interest for many years<sup>1-5</sup> not only because the reactions themselves display interesting chemistry, but also because they are involved in enzymic decarboxylation processes.<sup>6-9</sup> The catalytic mechanism

has been established to proceed via Schiff-base formation with the active species either being the protonated imine<sup>1b,10</sup> or one which has a labile proton so situated that it can be transferred to the nitrogen atoms as  $\text{CO}_2$  loss occurs.<sup>2</sup> The carboxylic acid

(1) (a) K. J. Pedersen, *J. Am. Chem. Soc.*, **51**, 2098 (1929); (b) *ibid.*, **60**, 595 (1938), and references cited therein.

(2) F. H. Westheimer and W. A. Jones, *J. Am. Chem. Soc.*, **63**, 3283 (1941).

(3) R. W. Hay, *Aust. J. Chem.*, **18**, 337 (1965).

(4) J. Peter Guthrie and Frank Jordan, *J. Am. Chem. Soc.*, **94**, 9136 (1972).

(5) Kazuo Taguchi and F. H. Westheimer, *J. Am. Chem. Soc.*, **95**, 7413 (1973).

(6) G. A. Hamilton and F. H. Westheimer, *J. Am. Chem. Soc.*, **81**, 6332 (1959); I. Fridovich and F. H. Westheimer, *ibid.*, **84**, 3208 (1962).

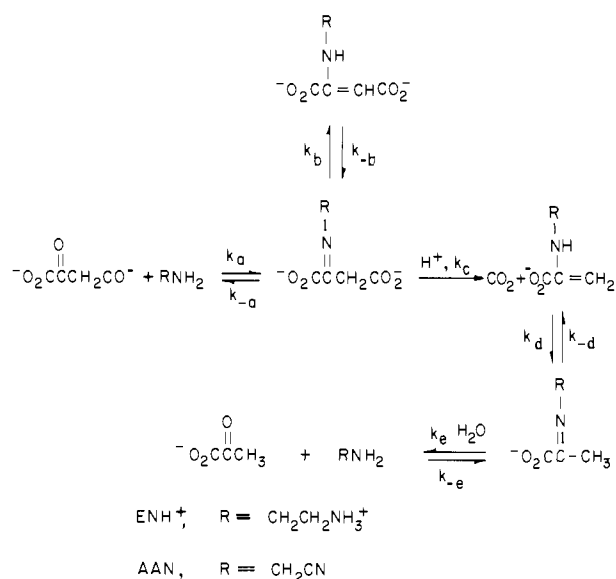
(7) F. H. Westheimer, *Proc. Chem. Soc., London*, 253 (1963).

(8) M. H. O'Leary and Richard L. Baughn, *J. Am. Chem. Soc.*, **94**, 626 (1972).

(9) D. E. Schmidt, Jr., and F. H. Westheimer, *Biochemistry*, **10**, 1249 (1971).

(10) W. P. Jencks, "Catalysis in Chemistry and Enzymology", McGraw-Hill, New York, 1969.

Scheme I



group that is lost very conveniently serves as such a proton donor site. A dead-end side reaction is conversion of the ketimine to enamine.<sup>4</sup> The reactions are summarized in Scheme I.

Here we report on a study of the decarboxylation of oxalacetate ( $\text{OA}^{2-}$ ) catalyzed by ethylenediamine (EN). This investigation was prompted by a report from Munakata et al.<sup>12</sup> that EN is a good catalyst for  $\text{CO}_2$  loss from  $\text{OA}^{2-}$ , while diamines in which the amine groups are separated by more than two carbon atoms are poorer catalysts. It was postulated<sup>12</sup> that enzyme catalysis may involve a sterically critical non-Schiff-base interaction between the amine groups and the carboxylate groups of  $\text{OA}^{2-}$ . Another possibility which we set out to explore is that  $\text{ENH}^+$ , which is a base of only moderate basicity, is the actual catalytically active form of EN. Aminoacetonitrile (AAN) has been shown<sup>4</sup> to be a potent catalyst for the decarboxylation of acetoacetate (AA), and in order to help bridge the gap between  $\text{OA}^{2-}$  and  $\text{AA}^-$  the AAN-catalyzed decarboxylation of  $\text{OA}^{2-}$  was also studied. A sufficiently wide range of conditions and rates were monitored so that it was possible to determine the protonation constants of the intermediates. The results provide reasons why weakly basic amines are better catalysts in this reaction than strongly basic ones.

### Experimental Section

Oxalacetic acid and 4-ethyloxalacetate, obtained from Nutritional Biochemical Corp., Cleveland, Ohio, were found respectively to be 98.1 and 98.2% pure by titration with standardized NaOH. They were stored under refrigeration and used without further purification. Aminoacetonitrile hydrochloride, obtained from Aldrich Chemicals, was recrystallized from 95% ethanol and standardized with NaOH. Ethylenediamine hydrochloride, obtained from Sigma Chemicals, was recrystallized from ethanol-water mixtures. Acetic acid, sodium hydroxide, and potassium chloride stock solutions were prepared in the usual manner. All experiments were carried out using double-distilled water. The ionic strength of all solutions was adjusted to 0.5 with KCl. All experiments were run at 25 °C. The pH of each solution was measured by using a Radiometer pH M26 pH meter after the glass electrode was standardized with NBS standard buffers.

The protonation constant of AAN was determined to be  $10^{5.51} \text{ M}^{-1}$ , (25 °C,  $I = 0.5$ ) by titration of a solution of the hydrochloride with standard NaOH. The  $\text{p}K_a$  values of  $\text{ENH}_2^{2+}$  were determined to be 7.18 and 10.18. The  $\text{p}K_a$ s of  $\text{H}_2\text{O}$ <sup>13</sup> were taken as reported in the literature.

(11) The abbreviations employed here:  $\text{OA}^{2-}$ , oxalacetate;  $\text{AA}^-$ , acetoacetate; AAN, aminoacetonitrile; EN, ethylenediamine;  $\text{OA}\cdot\text{EN}$ ,  $\text{OA}\cdot\text{AAN}$ , and  $\text{AA}\cdot\text{AAN}$ , the adducts formed by the reaction of  $\text{OA}^{2-}$  with EN and AAN, and  $\text{AA}^-$  with AAN, respectively. The absence of a subscript indicates the total adduct (the sum of ketimine, enamine, and possibly carbinolamine forms).

(12) M. Munakata, M. Matsui, M. Tabushi, and T. Shigematsu, *Bull. Chem. Soc. Jpn.*, **43**, 114 (1970).

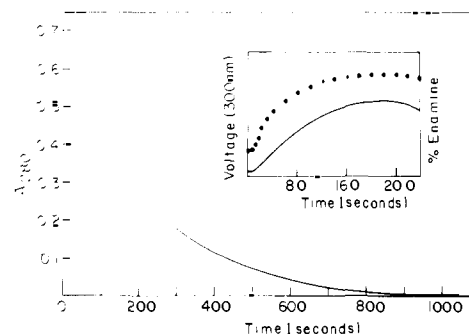


Figure 1. Absorbance-time traces observed during the reaction of oxalacetate with ethylenediamine,  $\text{EN}_{\text{tot}} = 0.050 \text{ M}$ ,  $\text{OA}_{\text{tot}} = 7.5 \times 10^{-4} \text{ M}$ , pH 6.09, 2.00-cm cell. Inset: —, stopped flow voltage trace; ....., calculated growth of enamine (offset for clarity).

4-Ethyloxalacetate (4-Et $\text{OA}^-$ ) is protonated in a pH region well below that investigated here and it was not necessary to determine the  $\text{p}K_a$  of its conjugate acid.

Absorption spectra for both slowly reacting and equilibrium solutions were obtained with a Cary 14 spectrophotometer equipped with a controlled temperature cell compartment. Faster absorbance changes were measured with a Durrum-Gibson stopped-flow apparatus interfaced to a minicomputer. Digitized absorbance values were logged at accurately determined time intervals. Manometric measurements were made with a Texas Instruments precision pressure gauge, 145-01.

Kinetic runs were made by mixing amine hydrochloride and  $\text{H}_2\text{O}$  $\text{A}$  solutions, each of which contained 0.05 M acetic acid, and were adjusted with NaOH to give the desired reaction pH after mixing. Each solution also contained sufficient KCl to give a final ionic strength of 0.5. Un-ionized  $\text{H}_2\text{O}$  $\text{A}$  is extensively hydrated in aqueous solutions<sup>14,15</sup> and, to obviate interference arising from dehydration over the first few seconds of the monitored reaction, the pH of the  $\text{H}_2\text{O}$  $\text{A}$  solution was brought to a pH well above  $\text{p}K_{1a}$  before mixing. The total amine was in sufficient excess over  $\text{OA}^{2-}$  that pseudo-first-order kinetics obtained.

Just as was observed by Guthrie and Jordan in the  $\text{AA}^-$ -AAN reaction,<sup>4</sup> three different rate processes are observed in the spectra after amine and  $\text{OA}^{2-}$  solutions are mixed. The fastest process (for which the observed pseudo-first-order rate constant is designated here as  $\lambda_1$ ) is manifested above pH 6 as an induction period. The second process ( $\lambda_2$ ) is seen either as an absorbance increase in the region 270–315 nm, where enamine absorbs, or as a decrease below 270 nm, where  $\text{OA}_{\text{en}}^{2-}$  absorbs. The time required for this intermediate process is 3–200 s, depending on conditions. The slower process ( $\lambda_3$ ) results in an absorbance decrease at all wavelengths longer than 240 nm; 5–200 min is required for completion. These three processes are evident in the absorbance-time curves shown in Figure 1.

For most rate determinations the enamine absorbance was monitored, but the wavelength of the maximum, 280 nm, was not suitable for following the growth of enamine because the catalyzed decrease in the  $\text{OA}^{2-}$  concentration strongly influenced the absorbance and prevented satisfactory "infinity time" absorbances from being obtained. By working in the 300–315-nm region this difficulty was overcome and satisfactory  $\lambda_{2,\text{obsd}}$  values resulted.  $\lambda_{3,\text{obsd}}$  values were conveniently measured by noting the absorbance decrease in the period after enamine had been formed.

The induction period was not observed below pH 6 owing to a rapid ketimine-enamine conversion rate compared to that of ketimine formation. Furthermore, even when observable, the induction period could not be measured with sufficient accuracy to warrant its use in the calculations. Owing to these difficulties,  $\lambda_1$  was not studied in detail.

The AAN catalysis system showed the same general spectral changes as were observed with EN, but the amplitude of the absorbance increase corresponding to enamine formation was smaller while the onset of decarboxylation was faster. As a result it was not possible to obtain satisfactorily accurate values for  $\lambda_{2,\text{obsd}}$  at any wavelength, and only the slow process could be followed with reasonable precision.

The data were analyzed by using computer programs based on the nonlinear curve-fitting algorithm described by Bevington.<sup>16,17</sup> In general,

(13) N. V. Raghavan and D. L. Leussing, *J. Am. Chem. Soc.*, **98**, 723 (1976).

(14) C. I. Pogson and R. G. Wolfe, *Biochem. Biophys. Res. Commun.*, **46**, 1048 (1972).

(15) F. C. Kokesh, *J. Org. Chem.*, **41**, 3593 (1976).

(16) Philip R. Bevington, "Data Reduction and Error Analysis for the Physical Sciences", McGraw-Hill, New York, 1969.

(17) V. S. Sharma and D. L. Leussing, *Talanta*, **18**, 1137 (1971).

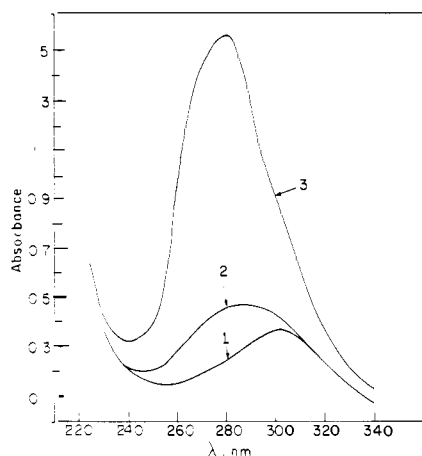


**Figure 2.** The absorption spectra of 4-ethyloxalacetate-ethylenediamine mixtures, 4-EtOA<sup>-</sup>  $1.5 \times 10^{-4}$  M: curve (EN<sub>TOT</sub>(M), pH) 1 (0, 4.96); 2 (0.10, 4.94); 3 (0.10, 7.78).

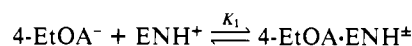
the absorbance-time curves for a system which displays two relaxations should be fit to the five-parameter equation  $Abs_t = Abs_\infty + A_1 \exp(-\lambda_1 t) + A_2 \exp(-\lambda_2 t)$ . Because the processes investigated here show widely disparate rates, it was permissible in most cases to omit the last term: all of the slow reactions adhered closely to the single exponential decay curve as also did those intermediate processes that approached a well-defined plateau.

Equilibrium absorbance data were analyzed by using a version of the curve-fitting program in which equilibrium distributions of all species and theoretical absorbances were calculated and compared with the observed. Pairs of equilibrium constants and molar absorptivities for the "unknowns" were varied in such a way as to give the best least-squares fit to the data. Another modification of the program was used to fit the rate data through the adjustment of the equilibrium and rate constants pertaining to a given trial reaction model.<sup>17</sup> A triple relaxation time subroutine was employed to analyze the rates obtained from the EN-OA studies. The details are provided in the Appendix.

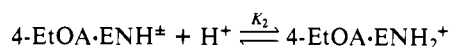
## Results

The absorbance changes which occur during the reaction of either AAN or EN or OA<sup>2-</sup> qualitatively resemble those observed by Guthrie and Jordan<sup>4</sup> for the reaction of AAN with AA<sup>-</sup>: an initial lag period is followed by an absorbance increase in the region of the enamine maximum, and this in turn is followed by an overall decrease. Manometric measurements confirm that  $\lambda_{3,obsd}$  determined from the rate of CO<sub>2</sub> release is identical with that obtained from the absorbance decrease. Reaction Scheme I, which has been proposed by Guthrie and Jordan,<sup>4</sup> is consistent with these observations.

**4-Ethyloxalacetate-Ethylenediamine.** The decarboxylation pathway is blocked with 4-EtOA<sup>-</sup> and it is a relatively easy matter to examine the equilibrium properties of solutions of amines with this substrate. Equilibrium absorption spectra in the presence and absence of 0.10 M EN total are shown in Figure 2. The development of a band centered at 280 nm in the presence of EN indicates the formation of enamine. At pH 7.8 this band becomes a dominant feature. The course of the 280-nm absorption as a function of the total EN concentration and pH is shown in Figure 3. Analysis of these data showed that the principal equilibria are



and



Values of  $K_1$ ,  $K_2$ , and the 280-nm molar absorptivities of these species are given in Table I. The solid lines drawn in Figure 3 are the theoretical absorbancies calculated by using these values.

The high 280-nm molar absorptivity of 4-EtOA<sup>-</sup>·ENH<sup>‡</sup> ( $\epsilon^{280} 1.05 \times 10^4 \text{ M}^{-1} \text{ cm}^{-1}$ ) lies close to values reported for  $\beta$ -cyanomethylcrotonate<sup>4</sup> ( $\epsilon^{280} 1.7 \times 10^4 \text{ M}^{-1} \text{ cm}^{-1}$ ) and OA<sup>2-</sup> enol<sup>18</sup> ( $\epsilon^{260}$

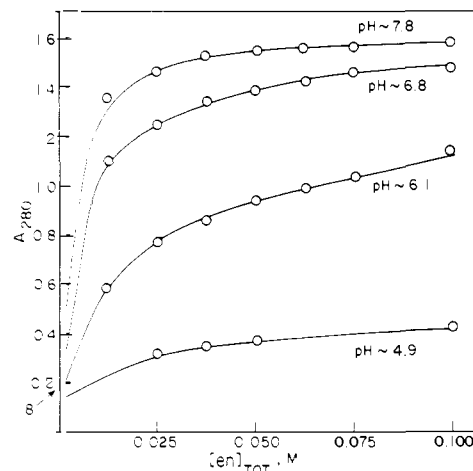


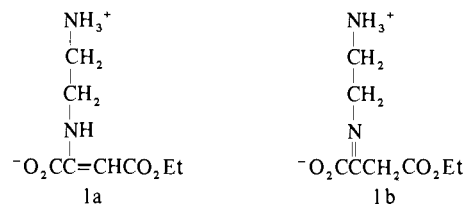
**Figure 3.** Absorbance of 4-ethyloxalacetate as a function of ethylenediamine concentration and pH,  $\lambda$  280 nm, 4-EtOA<sup>-</sup>  $1.50 \times 10^{-4}$  M, 2.00-cm cell. The solid lines are theoretical.

**Table I.** Rate and Equilibrium Constants for Adduct Formation: 4-Ethyloxalacetate and Ethylenediamine ( $I = 0.5$ , 25 °C)

reaction	constant
$4\text{-EtOA}^- + \text{ENH}^+ \xrightleftharpoons[k_{-1}]{k_1}$	$(\epsilon^{280} 1.05 \times 10^4) \log K_1 = 2.56,$
$4\text{-EtOA}\cdot\text{ENH}^\ddagger$	$k_1 = 0.11 \text{ M}^{-1} \text{ s}^{-1}$
$4\text{-EtOA}\cdot\text{ENH}^\ddagger + \text{H}^+ \xrightleftharpoons{\text{fast}}$	$(\epsilon^{280} 2.25 \times 10^3) \log K_2 = 5.37$
$4\text{-EtOA}\cdot\text{ENH}_2^+$	
$4\text{-EtOA}^- + \text{ENH}^+ + \text{H}^+ \xrightleftharpoons[k_{-2}]{k_2}$	$k_2 = 5.4 \times 10^5 \text{ M}^{-1} \text{ s}^{-1}$
$4\text{-EtOA}\cdot\text{ENH}_2^+$	
$\text{ENH}_2^{2+}$	$\text{p}K_{2a} = 7.18, \text{p}K_{2a} = 10.18$

$1.1 \times 10^4 \text{ M}^{-1} \text{ cm}^{-1}$ ) at their respective maxima. Close to 100% conversion of 4EtOA·ENH<sup>‡</sup> to enamine is indicated. Another manifestation of enamine formation is the high stability constant determined for this adduct since ketimines formed from aliphatic keto acids are usually found to have much lower stabilities.<sup>19</sup>

No evidence was obtained that the proton borne by the adduct ionizes under the conditions employed here. Therefore, its  $\text{p}K_a$  is at least 1.5 units larger than the highest pH investigated (7.8), placing it well in the range of aliphatic amine basicities. Owing to the interaction of the free electron pair of the secondary amine nitrogen atom with the conjugated  $\pi$  system of the OA<sup>2-</sup> moiety which is bound to it,<sup>4</sup> the secondary amine will be less basic than the terminal amine. The predominant form of the adduct therefore is the structure shown in **1a**. Since the conjugate acids of ketimine nitrogen atoms have  $\text{p}K_a$  values 4–5 units lower than that of the conjugate acid of the amine from which they are derived,<sup>10</sup> the terminal amine is also the dominant protonation site in the ketimine, **1b**.



**1a** is further protonated with an overall constant of  $10^{5.4} \text{ M}^{-1}$  to yield a diprotonated adduct which shows only 20% of the absorbance at 280 nm of the monoprotinated adduct. If only the enamines **2a'** and **2a''** contribute to this absorbance, it is unlikely that the remainder of the adduct is ketimine, because both the imine group and the 1-carboxylate group require considerably

(18) J. L. Hess and R. E. Reed, *Arch. Biochem. Biophys.*, **153**, 226 (1972).

(19) D. L. Leussing and D. C. Schultz, *J. Am. Chem. Soc.*, **86**, 4846 (1964).

## Scheme II

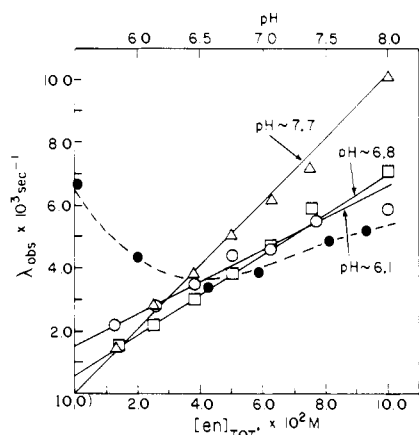
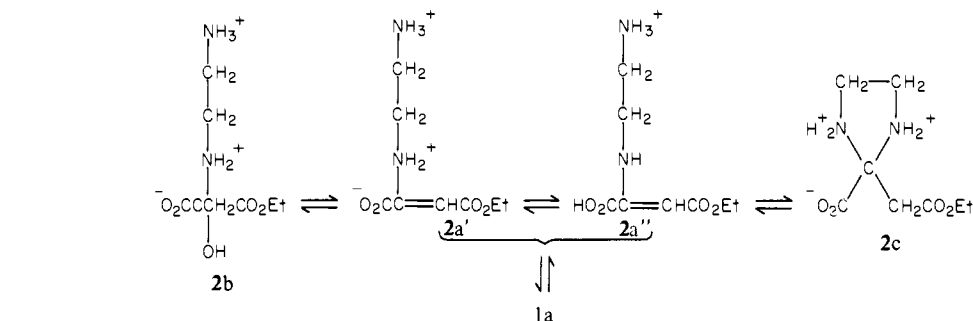


**Figure 4.** Observed pseudo-first-order rate constants for the formation of 4-ethyloxalacetate-ethylenediamine adducts,  $4\text{EtOA}^-$   $1.50 \times 10^{-4}$  M; —, varying  $[\text{EN}]_{\text{tot}}$  (O, pH 6.1; □, pH 6.8; Δ, pH 7.7); ---, varying pH; ●,  $[\text{EN}]_{\text{tot}}$  0.050 M. The solid lines and dashed lines are theoretical.

higher acidities for protonation. It is possible that the inductive effects of the two protons promote hydration to give a carbinolamine **2b**, or cyclization to give an imidazolidine, **2c** (Scheme II).

The known protonation properties of carbinolamines<sup>20</sup> and imidazolidines<sup>21</sup> are consistent with the proposed structures, and Hay<sup>3</sup> has found evidence for the formation of a stable carbinolamine in the reaction of aniline with 4-EtOA<sup>-</sup>. Figure 2 shows that the position of the absorption maximum of the adduct remains essentially unchanged when the diprotonated adduct is formed. If the extinction coefficient of **2a''**, in which the nitrogen atom lone electron pair participates in the extended chromophore, is the same as that of **1a**, then 20% of the diprotonated adduct is indicated to be present in this form. From this a  $pK_a$  of 4.7 is calculated for the ionization  $\text{2a}'' \rightleftharpoons \text{1a} + \text{H}^+$ .

On mixing  $4\text{EtOA}^-$  and EN solutions only one rate process, corresponding to the growth of enamine, was observed because decarboxylation cannot occur and ketimine  $\rightleftharpoons$  enamine conversion is fast with respect to the adduct formation rate. At a constant pH, the observed pseudo-first-order rate constants are seen in Figure 4 to be a linear function of total EN, as is expected for a reversible pseudo-first-order reaction. The rate equation which applies is

$$\lambda_{\text{obsd}} = k'[\text{EN}]_{\text{tot}} + k'' \quad (1)$$

At constant  $[\text{EN}]_{\text{tot}}$ ,  $\lambda_{\text{obsd}}$  exhibits a minimum at pH 6.5 (Figure 4).

Using the equilibrium constants determined spectrophotometrically the rate data of Figure 4 yielded the "solvent"- and proton-catalyzed paths:

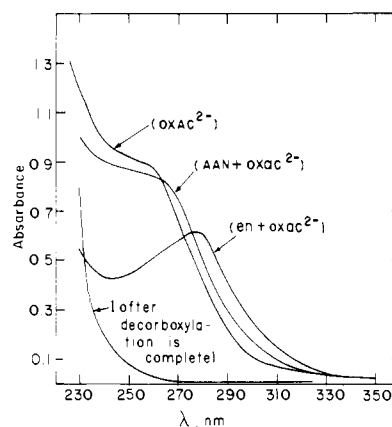
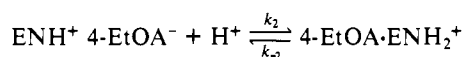
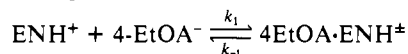


**Figure 5.** Preequilibrium and final absorption spectra of oxalacetate in the presence of ethylenediamine and aminoacetoneitrile:  $\text{OA}^{2-}$   $7.5 \times 10^{-4}$  M, pH 8.9; EN 0.050 M, pH 8.9; AAN 0.064 M, pH 6.9; 2.00-cm cell.

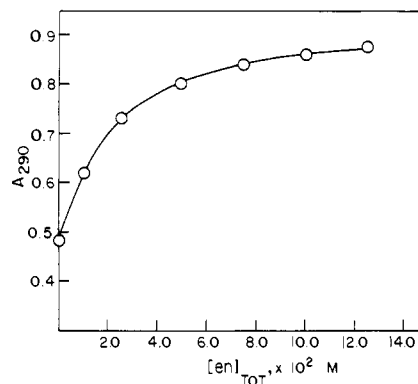


**Figure 6.** Variation of absorbance of oxalacetate preequilibrium solutions with ethylenediamine concentration,  $\text{OA}^{2-}$   $7.5 \times 10^{-4}$  M, pH 8.9 (buffered with 0.010 M *N,N,N',N'*-tetramethylethylenediamine), 2.00-cm cell.

The values found for the rate constants are given in Table I. These paths are typical of those found for Schiff-base formation between aliphatic keto acids and amines, and indeed the rate constants found here are close to those previously reported for the reaction of pyruvate with glycinate.<sup>22</sup>

**Oxalacetate-Ethylenediamine.** Above pH 7.5, rates of  $\text{CO}_2$  evolution become sufficiently slow with respect to those of adduct formation and tautomerization that a metastable preequilibrium position is reached shortly after the reactants are mixed. This permits stabilities to be determined independently of the kinetic determinations.

In Figure 5 are shown spectra of  $\text{OA}^{2-}$  solutions at pH 8.9 before the addition of EN, in the presence of EN after the metastable preequilibrium position has been attained but before decarboxylation became significant, and at the end of the decarboxylation process. The spectrum of  $\text{OA}^{2-}$ , with shoulder at 280 nm due to enol, is seen to be converted by EN to a spectrum which displays a prominent enamine band centered at 278 nm.

(20) Roland G. Kallen and W. P. Jencks, *J. Biol. Chem.*, **241**, 5864 (1966).

(21) A. Hilton and D. L. Leussing, *J. Am. Chem. Soc.*, **93**, 6831 (1971).

(22) D. L. Leussing and L. Anderson, *J. Am. Chem. Soc.*, **91**, 4698 (1969).

Table II. Observed and Calculated Pseudo-First-Order Rate Constants ( $s^{-1}$ ) for Decarboxylation: Oxalacetate and Ethylenediamine ( $I = 0.5$ ,  $25^\circ\text{C}$ ,  $7.5 \times 10^{-4}$  M OA Initially)

EN <sub>tot</sub>	pH	$\lambda_{1,obsd}$	calcd		
			$\lambda_3$	$\lambda_2$	$\lambda_1$
A. Slowest Rates					
0.025	4.00	0.0019	0.0017	0.6500	6.66
0.050	4.06	0.0036	0.0035	0.6793	6.47
0.075	4.06	0.0051	0.0052	0.6794	6.47
0.100	3.98	0.0062	0.0066	0.6403	6.72
0.025	5.08	0.0025	0.0021	0.9336	3.67
0.055	5.02	0.0045	0.0047	0.9711	3.64
0.075	5.05	0.0061	0.0064	0.9543	3.65
0.100	5.11	0.0081	0.0085	0.9152	3.69
0.025	5.63	0.0029	0.0022	0.4146	5.60
0.050	5.58	0.0050	0.0045	0.4610	5.30
0.075	5.64	0.0066	0.0067	0.4125	5.62
0.100	5.65	0.0079	0.0089	0.4040	5.68
0.025	6.22	0.0028	0.0024	0.1253	8.97
0.050	6.09	0.0042	0.0047	0.1651	8.26
0.075	6.29	0.0069	0.0073	0.1085	9.33
0.100	6.09	0.0085	0.0094	0.1651	8.28
0.025	6.46	0.0032	0.0026	0.0759	10.06
0.050	6.40	0.0057	0.0050	0.0875	9.79
0.075	6.46	0.0076	0.0075	0.0770	10.07
0.100	6.58	0.0100	0.0100	0.0625	10.48
0.025	7.05	0.0031	0.0028	0.0251	11.55
0.050	6.99	0.0053	0.0052	0.0294	11.46
0.075	7.04	0.0062	0.0069	0.0300	11.53
0.100	7.04	0.0070	0.0084	0.0328	11.53
0.025	7.47	0.0024	0.0020	0.0155	11.94
0.050	7.41	0.0027	0.0037	0.0200	11.90
0.075	7.42	0.0034	0.0043	0.0244	11.91
0.025	7.93	0.0010	0.0009	0.0128	12.10
0.050	7.90	0.0013	0.0014	0.0185	12.09
0.075	7.90	0.0015	0.0017	0.0243	12.09
0.100	7.94	0.0015	0.0017	0.0303	12.10
0.025	8.68	0.0002	0.0003	0.0117	12.17
0.050	8.68	0.0002	0.0004	0.0181	12.17
0.038	8.88	0.0002	0.0003	0.0148	12.18
0.075	8.84	0.0002	0.0003	0.0244	12.18
B. Intermediate Rates					
0.050	3.59	0.45	0.0027	0.4534	7.48
0.075	3.57	0.50	0.0040	0.4457	7.50
0.100	3.56	0.50	0.0053	0.4420	7.51
0.075	4.01	0.59	0.0051	0.6564	6.62
0.100	4.02	0.62	0.0068	0.6608	6.59
0.050	4.48	0.83	0.0039	0.8842	4.91
0.075	4.51	0.87	0.0059	0.8964	4.82
0.100	4.51	0.92	0.0079	0.8986	4.80
0.075	5.04	1.10	0.0064	0.9617	3.64
0.050	5.14	0.90	0.0043	0.8889	3.74
0.100	5.06	1.00	0.0085	0.9476	3.65
0.050	5.56	0.44	0.0045	0.4777	5.20
0.075	5.52	0.49	0.0066	0.5138	5.00
0.100	5.53	0.47	0.0088	0.5024	5.06
0.038	6.07	0.17	0.0036	0.1719	8.15
0.050	6.02	0.19	0.0047	0.1922	7.84
0.075	6.05	0.20	0.0070	0.1811	8.02
0.100	6.04	0.21	0.0093	0.1850	7.96
0.038	6.46	0.062	0.0039	0.0759	10.07
0.050	6.47	0.060	0.0051	0.0754	10.09
0.075	6.50	0.070	0.0075	0.0716	10.21
0.100	6.50	0.065	0.0099	0.0725	10.21
0.038	6.94	0.031	0.0041	0.0311	11.37
0.050	6.95	0.035	0.0052	0.0313	11.39
0.075	6.94	0.032	0.0073	0.0338	11.37
0.100	6.92	0.033	0.0094	0.0369	11.33
0.025	7.93	0.012	0.0011	0.0126	12.10
0.050	7.90	0.018	0.0015	0.0185	12.09

Both of these features disappear when decarboxylation is complete.

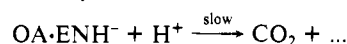
A plot of the preequilibrium absorbance at 290 nm as a function of total EN at pH 8.9 is shown in Figure 6. Analysis of these results yielded a value of  $49 \text{ M}^{-1}$  for the equilibrium constant of the reaction



From this value about 70% of the total  $\text{OA}^{2-}$  is calculated to be converted to adduct in the preequilibrium solution shown in Figure 5. From the absorbance at 278 nm, a molar absorptivity of  $1.0 \times 10^3 \text{ M}^{-1} \text{ cm}^{-1}$  is obtained for the adduct at its absorption maximum. Depending on the molar absorptivity assumed for the enamine and assuming that ketimine absorbance is negligible, about 6–10% of  $\text{OA}\cdot\text{ENH}^-$  is indicated to be present as enamine. The stability constant of this adduct, which is about  $1/5$  as large as that of the ester, is also consistent with a predominant ketimine content.

Rate determinations were made over a range of pH and total EN concentrations. The experimental conditions and corresponding rate constants found for the slow process,  $\lambda_{3,obsd}$ , are given in Table IIA and the data pertaining to the intermediate rates,  $\lambda_{2,obsd}$ , are given in Table IIB.

Both the  $\lambda_{2,obsd}$  and  $\lambda_{3,obsd}$  exhibit pH maxima lying at 5.0 and 6.5, respectively. The  $\lambda_{2,obsd}$  are insensitive to  $[\text{EN}]_{\text{tot}}$  but the  $\lambda_{3,obsd}$  are strongly dependent on it. Above pH 7.5 this dependency is quantitatively described by the preequilibrium formation of  $\text{OA}\cdot\text{ENH}^-$  according to eq 2, followed by rate-determining proton-assisted decarboxylation:



In the acidic pH region, the preequilibrium model failed to account satisfactorily for the observations, and rate-limiting imine formation was indicated. Further data analysis was performed by using an expanded reaction model based on Scheme I but to which were appended fast protonation reactions involving enamine and ketimine. Estimates of the protonation constants of the various basic groups for these species were made on the following basis. The terminal amine group was assumed to remain protonated and the 1-carboxylate group of the  $\text{OA}^{2-}$  moiety unprotonated throughout the investigated pH range. The  $\text{p}K_a$  of the iminium group was taken as 3.0, a value less than  $\text{p}K_{1a}$  of  $\text{ENH}_2^{2+}$  by an amount which is the average of the expected decrease of 4.0–5.0 pK units.<sup>10</sup> The  $\text{p}K_a$  of the 4-carboxylic acid group of the ketimine was initially assumed to be slightly higher than  $\text{p}K_{2a}$  of  $\text{H}_2\text{OA}$  (4.0), and this estimate was refined in the curve-fitting procedures. For this group in the enamine a value of around 5.0 was initially taken, in view of a  $\text{p}K_a$  of 5.4 estimated by Guthrie and Jordan<sup>4</sup> for *trans*- $\text{CH}_3\text{C}(\text{NH}_2)=\text{CHCO}_2\text{H}$ . This value was also refined during the curve-fitting process. Owing to the possibility of H bonding between the secondary amine of the enamine and the 4- $\text{CO}_2\text{H}$  group, the  $\text{p}K_a$  of the enammonium group was taken as 3.5, a value about 1 pK<sub>a</sub> unit lower than that reported above for the enamine ester adduct. Owing to the insensitivity of the calculations to the  $\text{p}K_a$  values of 4 and lower, substantial errors in these estimates could be tolerated without significantly influencing the conclusions given below. The stability constant of  $\text{OA}\cdot\text{ENH}_{\text{imine}}^-$ ,  $K_3$ , was also taken as  $49 \text{ M}^{-1}$  and the  $\text{OA}\cdot\text{ENH}_{\text{enamine}}^-/\text{OA}\cdot\text{ENH}_{\text{ketimine}}^-$  ratio,  $R_1$ , was assumed to be 0.06.

After repeated trials using various test reaction models, the reaction scheme presented in Table III was obtained. Commonly, when as large a number of rate parameters as has been determined here is sought from the concentration dependence of a measured physical phenomenon, ill conditioning in the set of equations to be solved introduces large uncertainties into the final values unless highly precise data points are available. In the present study the acquisition of coupled data sets over two different time domains improved the conditioning considerably. The necessity to accommodate the different pH maxima and EN concentration dependencies imposed stringent requirements on the numerical solution. The "best" values given in Table III showed deviations of 10–30% for the equilibrium constants and 30–50% for the rate constants.

The salient features of the proposed reaction scheme are summarized as follows.

(1) The rate law for the reaction of  $\text{OA}^{2-}$  and  $\text{ENH}^+$  to yield ketimine is identical with that found above for ester adduct formation, with the rate constants being only slightly higher in the case of  $\text{OA}^{2-}$ . In the experiments performed in the lower pH region, a contribution to the rate from the proton-catalyzed re-

Table III. Rate and Equilibrium Constants: Oxalacetate and Ethylenediamine ( $I = 0.5$ ,  $25^\circ\text{C}$ )

reaction	constant
$\text{OA}^{2-} + \text{ENH}^+ \xrightleftharpoons{k_3} \text{OA}\cdot\text{ENH}_{\text{imine}}^-$	$\log K_3 = 1.69,^a$ $k_3 = 0.27 \text{ M}^{-1} \text{ s}^{-1}$
$\text{OA}\cdot\text{ENH}_{\text{imine}}^- + \text{H}^+ \xrightleftharpoons{\text{fast}} \text{OA}\cdot\text{ENH}_{2,\text{imine}}$	$\log K_4 = 4.5$
$\text{OA}\cdot\text{ENH}_{2,\text{imine}} + \text{H}^+ \xrightleftharpoons{\text{fast}} \text{OA}\cdot\text{ENH}_{3,\text{imine}}^+$	$\log K_5 \sim 3.0$
$\text{OA}^{2-} + \text{ENH}^+ + \text{H}^+ \xrightarrow{k_4} \text{OA}\cdot\text{ENH}_{2,\text{imine}}$	$k_4 = 1.7 \times 10^6 \text{ M}^{-2} \text{ s}^{-1}$
$\text{HOA}^- + \text{ENH}^+ + \text{H}^+ \xrightarrow{k_5} \text{OA}\cdot\text{ENH}_{3,\text{imine}}^+$	$k_5 = 1.1 \times 10^6 \text{ M}^{-2} \text{ s}^{-1}$
$\text{OA}\cdot\text{ENH}_{\text{imine}}^- \xrightleftharpoons[k_{-6}]{k_6} \text{OA}\cdot\text{ENH}_{\text{enamine}}^-$	$R_1 = 0.06,^a$ $k_6 = 1 \text{ s}^{-1}$
$\text{OA}\cdot\text{ENH}_{2,\text{imine}} \xrightleftharpoons[k_{-7}]{k_7} \text{OA}\cdot\text{ENH}_{2,\text{enamine}}$	$R_2 = 1.4,^b$ $k_7 = 0.6 \text{ s}^{-1}$
$\text{OA}\cdot\text{ENH}_{\text{enamine}}^- + \text{H}^+ \xrightleftharpoons{\text{fast}} \text{OA}\cdot\text{ENH}_{2,\text{enamine}}$	$\log K_6 = 5.8$
$\text{OA}\cdot\text{ENH}_{2,\text{enamine}} + \text{H}^+ \xrightleftharpoons{\text{fast}} \text{OA}\cdot\text{ENH}_{3,\text{enamine}}^+$	$\log K_7 \sim 3.5$
$\text{OA}\cdot\text{ENH}_{2,\text{imine}} \xrightarrow{k_8} \text{CO}_2 + \dots$	$k_8 = 6 \text{ s}^{-1}$

<sup>a</sup> Determined from spectrophotometric equilibrium measurements. <sup>b</sup> Calculated using eq 13a in the Appendix.

action of  $\text{ENH}^+$  with  $\text{HOA}^-$  was also observed.

(2) The protonation constant of  $\text{OA}\cdot\text{ENH}_{\text{imine}}^-$ ,  $K_4$ , is about  $10^{4.5} \text{ M}^{-1}$ , a value entirely consistent with protonation at the  $4\text{-CO}_2^-$  group and not at the  $>\text{C}=\text{N}$  group. The protonation constant,  $K_6$ , of  $\text{OA}\cdot\text{ENH}_{\text{enamine}}^-$  is found to be around  $10^{5.8} \text{ M}^{-1}$ , which is also consistent with the site being the  $4\text{-CO}_2^-$  group. In the latter structure the higher basicity arises from the transfer of electron density to the carboxylate group via the conjugated  $\pi$  system.<sup>4</sup> It was also found that the result obtained for this protonation constant depends on the value assumed for  $R_1$ ; e.g., a factor of 2 increase in  $R_1$  causes a corresponding decrease in  $K_6$ . Owing to the uncertainty in  $R_1$ ,  $K_6$  can only be said to lie in the region  $10^{5.6}\text{--}10^{5.8} \text{ M}^{-1}$ . An important consequence of finding  $K_6 \gg K_4$  is that  $R_2 \gg R_1$ , where  $R_2$  is the enamine/ketimine ratio of the diprotonated adduct. Because enamine formation competes with decarboxylation, the increase in enamine concentration on protonation causes net rates of  $\text{CO}_2$  loss to be slow.

(3)  $\text{OA}\cdot\text{ENH}_{2,\text{imine}}$  is essentially the only species that undergoes decarboxylation. The proton on the terminal ammonium group is too tightly bound to aid the decarboxylation of the mono-protonated imine, and with the triprotonated imine  $\text{CO}_2$  loss is inhibited by the absence of a suitable site to which the  $4\text{-CO}_2\text{H}$  proton can be transferred.

(4) The rate of ketimine  $\rightleftharpoons$  enamine conversion is sufficiently slow in the higher pH region investigated that this rate could be measured. At lower pH, the rate of ketimine formation is rate limiting, and tautomerization becomes essentially equivalent to a coupled equilibrium process. Thus, it was possible to obtain the tautomerization rates of  $\text{OA}\cdot\text{ENH}_{\text{imine}}^-$  and  $\text{OA}\cdot\text{ENH}_{2,\text{imine}}$  but not that of  $\text{OA}\cdot\text{ENH}_{3,\text{imine}}^+$ .

Using the values given in Table II, the theoretical values of the three relaxation rate constants for each set of reaction conditions have been computed and are given in Table II. Good overall agreement between  $\lambda_{3,\text{obsd}}$  and  $\lambda_{3,\text{calcd}}$  in Table IIA and between  $\lambda_{2,\text{obsd}}$  and  $\lambda_{2,\text{calcd}}$  in Table IIB is seen to be achieved.

As an independent check on the model, a numerical integration was performed for the reaction conditions employed in obtaining the absorbance-time curves shown in Figure 1. The dotted curve showed in the inset of Figure 1 describes the calculated time dependence on the enamine scaled to match the amplitude of the absorbance trace. Even though induction period times were not employed in the curve fitting, it is seen this initial time lag and the following rates of absorbance increases are reproduced very well. The enamine concentration does not decrease as fast as the

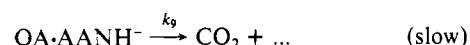
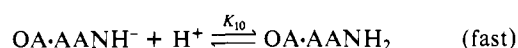
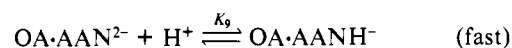
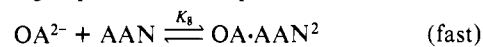
absorbance at longer times because the decreasing concentration of free  $\text{OA}^{2-}$  in solution influences the absorbance readings.

Esters of  $\beta$ -keto acids, because they do not decarboxylate, have been employed as models for estimating the stabilities and rates of formation of the amine adducts of the unesterified acids.<sup>3,4,23</sup> The assumption justifying this procedure is that the remote ester group has only a slight influence on the substituent in the  $\beta$  position. This certainly is reasonable with respect to the ketimine, but the present results show that the ester adduct has a great proclivity to transform to the enamine and this causes the overall stability of the ester adduct to be considerably higher than that of the unesterified acid. Differences in stabilities will also influence the observed rates of equilibration. According to eq 1, if two different reversible systems show identical forward reaction rates, that having the larger backward rate (lower stability) will equilibrate faster. This effect will cause the observed rates of equilibration of the more stable esters to appear to be slower than those of the unesterified acids even though the forward rates in these two systems are nearly identical. It is important to factor out these influences of enamine on stabilities and rates before drawing conclusions regarding the acids when the esters are used as models.

**Oxalacetate-Aminoacetonitrile.** The AAN- $\text{OA}^{2-}$  reaction system displays absorbance changes that are similar to those described above for  $\text{ENH}^+$  catalysis. Above pH 5.5 an induction period of about 1 s is followed by an absorbance increase in the near-UV which takes 5–30 s for completion. These changes in turn are followed by an absorbance decrease that is accompanied by  $\text{CO}_2$  evolution. Qualitatively similar changes were described by Guthrie and Jordan<sup>4</sup> in their investigation of the AAN-AA<sup>-</sup> reaction system. Major quantitative differences exist between the  $\text{OA}^{2-}$  and the AA<sup>-</sup> reactions, however. In the  $\text{OA}^{2-}$  reaction the induction period is about ten times longer, but the rate of absorbance decrease (decarboxylation) is ten times faster. Furthermore, the amplitude of the intermediate absorbance increase is smaller in the case of  $\text{OA}^{2-}$ . A small amplitude followed by fast decarboxylation prevented the acquisition of sufficiently accurate values of  $\lambda_{2,\text{obsd}}$  to warrant their use in the calculations. Only the  $\lambda_{3,\text{obsd}}$  values were subjected to the curve-fitting procedures.

Figure 5 displays a spectrum of  $\text{OA}^{2-}$  in a solution containing 0.06 M AAN buffered about 1 pH unit above the  $\text{p}K_a$  of  $\text{HAAN}^+$ . This spectrum was taken during the interval after adduct formation was complete and before significant  $\text{CO}_2$  loss occurred. No evidence of an enamine absorption band is observed at 280 nm. Calculations using the equilibrium constants determined below reveal that 20% of the  $\text{OA}^{2-}$  is converted to  $\text{OA}\cdot\text{AAN}^{2-}$ , of which possibly no more than 10% is present as enamine. The stopped flow absorbance changes indicate that enamine is actually formed, but the low amplitude confirms that the amount is relatively small.

Values of  $\lambda_{3,\text{obsd}}$  for various reaction conditions are presented in Table IV. In contrast to the results obtained with  $\text{ENH}^+$ , the AAN data were found to conform to a preequilibrium reaction sequence, involving unprotonated and protonated adducts.



The calculated values of the rate and equilibrium constants for these reactions are given in Table IV along with the theoretical  $\lambda_{3,\text{calcd}}$ .

The stability constant of  $\text{OA}\cdot\text{AAN}^-$  ( $K_8$  of Table IV) is seen to be appreciably smaller than that of  $\text{OA}\cdot\text{ENH}^-$  ( $K_3$ ), reflecting both the lower basicity of AAN and the low enamine content of the adduct. The overall protonation constant of this AAN adduct

Table IV. Overall Rate and Equilibrium Constants: Oxalacetate and Aminoacetonitrile ( $I = 0.5$ ,  $25^\circ\text{C}$ )

reaction		constant	
$\text{OA}^{2-} + \text{AAN} \xrightleftharpoons{\text{fast}} \text{OA}\cdot\text{AAN}^{2-}$		$\log K_8 = 0.32$	
$\text{OA}\cdot\text{AAN}^{2-} + \text{H}^+ \xrightleftharpoons{\text{fast}} \text{OA}\cdot\text{AANH}^+$		$\log K_9 = 4.6$	
$\text{OA}\cdot\text{AANH}^+ + \text{H}^+ \xrightleftharpoons{\text{fast}} \text{OA}\cdot\text{AANH}_2$		$\log K_{10} = 3.0$	
$\text{OA}\cdot\text{AANH}^+ \xrightarrow{k_9} \text{CO}_2 + \dots$		$k_9 = 1 \text{ s}^{-1}$	
AANH: $\text{p}K_a = 5.51$			
AAN <sub>tot</sub>	pH	$\lambda_{\text{obsd}}$	$\lambda_{\text{calcd}}$
0.024	4.121	0.0030	0.0029
0.048	4.229	0.0062	0.0063
0.072	4.019	0.0088	0.0079
0.096	3.849	0.0086	0.0086
0.144	4.039	0.0131	0.0159
0.022	4.586	0.0035	0.0034
0.044	4.564	0.0068	0.0068
0.022	4.961	0.0030	0.0034
0.044	4.965	0.0065	0.0066
0.065	4.964	0.0094	0.0097
0.089	4.947	0.0124	0.0132
0.133	4.925	0.0151	0.0194
0.022	5.529	0.0027	0.0022
0.044	5.481	0.0053	0.0046
0.066	5.529	0.0076	0.0064
0.089	5.481	0.0097	0.0090
0.023	5.975	0.0011	0.0012
0.046	6.093	0.0020	0.0019
0.069	6.005	0.0031	0.0033
0.092	6.092	0.0037	0.0036
0.138	6.025	0.0058	0.0058
0.030	6.913	0.0003	0.0002
0.045	6.788	0.0005	0.0005
0.060	7.004	0.0004	0.0004
0.074	7.082	0.0004	0.0004

( $K_9$ ) is considerably lower than that of  $\text{OA}\cdot\text{ENH}_{\text{enamine}}^-$ ,  $10^{4.6} \text{ M}^{-1}$  compared to  $10^{5.8} \text{ M}^{-1}$ , but is close to that of  $\text{OA}\cdot\text{ENH}_{\text{imine}}^-$ ,  $10^{4.5} \text{ M}^{-1}$ . That this value lies in the vicinity of the value expected for the protonation of the 4-CO<sub>2</sub><sup>-</sup> group of the ketimine implies that the enamine content of the monoprotonated adduct is also low. With AAN, enamine formation does not appear to interfere appreciably with the decarboxylation of the  $\text{OA}^{2-}$  adduct.

### Discussion

Both  $\text{ENH}^+$  and AAN are found here to be effective catalysts for the decarboxylation of  $\text{OA}^{2-}$ . Comparing rates at the pH maxima, AAN-catalyzed decarboxylation is 50% faster than that of  $\text{ENH}^+$ , while aniline at its pH 4.0 maximum at  $30^\circ\text{C}$  is only slightly faster than  $\text{ENH}^+$  at  $25^\circ\text{C}$ . At pH 5.0, AAN decarboxylates  $\text{OA}^{2-}$  about ten times faster than  $\text{AA}^-$ .

The present results support the general mechanism proposed by Guthrie and Jordan<sup>4</sup> for the AAN-catalyzed CO<sub>2</sub> loss with  $\text{AA}^-$ ; however, differences exist between their system and the  $\text{OA}^{2-}$  reactions studied here.  $\text{OA}^{2-}$  reacts faster with the amine and forms a more stable ketimine.  $\text{OA}^{2-}$  also forms less enamine and the tautomerization proceeds at a slower (albeit still relatively fast) rate. These differences are the primary cause of faster rates of CO<sub>2</sub> evolution from  $\text{OA}^{2-}$  because the absolute rate constants for this process in these two systems lie fairly close to each other. The values are 6, 1, and  $10 \text{ s}^{-1}$  for the decarboxylation of  $\text{OA}\cdot\text{ENH}_{2,\text{imine}}^-$ ,  $\text{OA}\cdot\text{AANH}^+$ , and  $\text{AA}\cdot\text{AANH}_{\text{imine}}^-$ , respectively. The low value given for  $\text{OA}\cdot\text{AANH}^+$  has not been corrected for the presence of the presumably small amount of enamine. It is important to note that these rate constants are insensitive to the differences in the basicities of the parent amines, and certainly do not reflect the 50-fold ratio in the  $\text{ENH}^+:\text{AAN}$  protonation constants.

The protonation steps involved in the reaction sequence are complicated and influence the rates at each stage; nevertheless, reasons why weakly basic amines are better catalysts than strongly basic amines emerge from the present study. To illustrate these

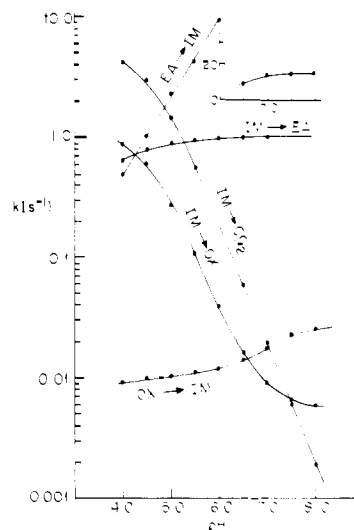


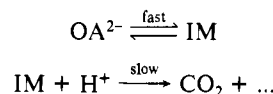
Figure 7. pH dependency of the effective rate constants in 0.10 M  $\text{EN}_{\text{tot}}$ .

points the effective first-order, pH-dependent rate constants for the individual steps involved in the catalyzed decarboxylation of  $\text{OA}^{2-}$  have been calculated for a medium containing 0.10 M total EN, and are shown plotted in Figure 7. First, it can be seen that the rate of conversion of  $\text{OA}^{2-}$  to IM (imine) is slow at pH 4.0, but increases somewhat as the pH increases to the region where the simple second-order reaction between  $\text{OA}^{2-}$  and  $\text{ENH}^+$  prevails. Pertinent to the discussion below, it should be noted that, although the rate law given in Table III shows terms for proton catalysis, these pathways do not cause an acceleration in the imine formation rate because they are influential in the pH region where EN is essentially completely present in the diprotonated form. Here, the concentration of the active form,  $\text{ENH}^+$ , varies inversely with  $[\text{H}^+]$ , so that the product  $[\text{H}^+][\text{ENH}^+]$  is a constant.

Decarboxylation of IM is seen to be fast at pH 4.0 but the rates of the competing reactions,  $\text{IM} \rightarrow \text{OA}^{2-}$  and  $\text{IM} \rightarrow \text{EA}$  (enamine), lie sufficiently close that appreciable amounts of IM are lost along these routes before decarboxylation occurs. Nevertheless, it can be accurately said that in the low-pH region the rate of formation of imine is the rate-limiting step for decarboxylation.

At pH 4.0 it should also be noted that  $\text{EA} \rightarrow \text{IM}$  is slower than  $\text{IM} \rightarrow \text{EA}$ . This is a manifestation of the increase in stability which occurs when the relatively basic enamine is protonated. The enamine/ketimine ratio of  $\text{OA}\cdot\text{ENH}_2$  is greater than unity in contrast to the small ratio found with  $\text{OA}\cdot\text{ENH}^-$ .

As the reaction pH is increased, the rates of the  $\text{OA}^{2-} \rightarrow \text{IM}$  and  $\text{IM} \rightarrow \text{EA}$  reactions change only slightly but the rates of the back reaction,  $\text{IM} \rightarrow \text{OA}^{2-}$ , and decarboxylation,  $\text{IM} \rightarrow \text{CO}_2$ , show pronounced decreases. Furthermore, the rate  $\text{EA} \rightarrow \text{IM}$  increases sharply reflecting the greater part of the destabilization of the enamine as the 4-CO<sub>2</sub>H proton is dissociated. Above pH 8 the reaction system can be approximated satisfactorily by the simplified scheme



Although the imine formation rate constants have not been determined for the reaction of  $\text{OA}^{2-}$  with AAN, it is reasonable to assume that they do not differ very much from those found for the reaction of  $\text{OA}^{2-}$  with EN. The semiquantitatively similar relaxation times observed with the two amines support this assumption, as do earlier results obtained in our laboratory<sup>24</sup> which show that the rate constants for the formation of salicylaldehyde imines are independent of the amine basicity. In other studies, however, Hine and Via<sup>25</sup> found that rate constants for the reactions

(24) D. L. Leussing, "Metal Ions in Biological Systems", Vol. 5, H. Sigel, Ed., Marcel Dekker, New York, 1976.

(25) J. Hine and F. A. Via, *J. Am. Chem. Soc.*, **94**, 190 (1972).

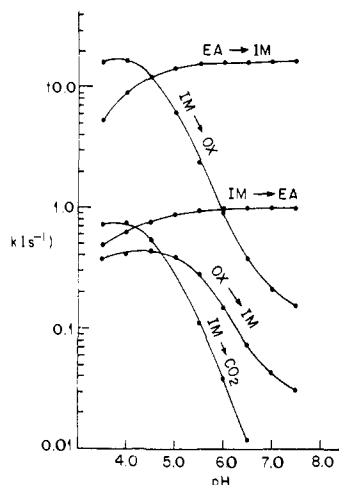


Figure 8. pH dependency of the effective rate constants in 0.10 M AAN<sub>tot</sub>.

of various amines with isobutyraldehyde do decrease with amine basicity but the change is less than that of the dissociation constants of the conjugate acids. Most importantly for the present argument, in both the isobutyraldehyde<sup>25</sup> and salicylaldehyde<sup>24</sup> cases, the rate constants for the proton-catalyzed steps were found to depend very little on the amine basic strength.

The results of computations of the effective rate constants for the AAN-OA<sup>2-</sup> system are presented in Figure 8. The same rate law and rate constants for the paths OA<sup>2-</sup> → IM and IM → EA as found for the EN system were employed, but the equilibrium constants given in Table IV were used to obtain the rate constants for the back reactions. The rate constant for the decarboxylation of the monoprotonated adduct given in Table IV was also used.

Although the curves drawn in Figure 8 may differ slightly from the actual ones, a comparison with Figure 7 reveals features which shed light on amine catalysis in general. For one, in the AAN system, the high rate of the EA → IM back reaction assures that the extent of enamine formation will be negligible and not affect decarboxylation even though the IM → EA rate may lie close to that for CO<sub>2</sub> loss in the more acidic media. With the more basic EN, on the other hand, stabilization of the enamine via protonation does cause interference with decarboxylation. It is expected that the greater enamine basicity which arises from the formation of adducts with even more basic amines<sup>26</sup> would cause the curve for the EA → IM rate to be displaced further downward with respect to the curves for EA formation and IM decarboxylation. We propose that it is this increased interference from enamine formation that accounts for the low catalytic effect observed for highly basic amines in this type of decarboxylation reaction. This type of interference may not be as critical in an enzyme where the structure around the active site may favor the binding of ketimine over enamine. Results obtained in our laboratories<sup>27</sup> show that pyruvate kinase, which possesses OA<sup>2-</sup> decarboxylase activity, differentiates strongly between the keto and enol forms of the substrate.

The lower amount of enamine formed by the AAN adduct of OA<sup>2-</sup> only accounts for a small part of its faster decarboxylation rate, however. The major part of the higher catalytic efficacy of AAN compared to EN arises from the faster OA<sup>2-</sup> → IM rate observed with the former. Even though the same rate constants were used to calculate these rates in the two cases, the rate profiles show remarkably different behavior: the IM formation rates with EN show a slight decrease on going from high pH to low pH, but those for AAN show a pronounced increase. This difference arises because the term for proton catalysis becomes important in a region where significant concentrations of AAN remain unprotonated, whereas, as discussed above, in this same region the

ENH<sup>+</sup> concentration varies inversely with the H<sup>+</sup> concentration and negates the effects of an increase in the latter.

Spetnagel and Klotz<sup>23</sup> have observed catalytic decarboxylation of OA<sup>2-</sup> by partially quaternized poly(ethylenimine) having 10% primary amine residues. The reaction shows the characteristics of amine catalysis; e.g., the pH-rate profile is bell shaped, but no evidence of enamine formation in the presence of OA<sup>2-</sup> was observed. Saturation kinetics were found, yielding an OA<sup>2-</sup> Michaelis binding constant of  $3.5 \times 10^{-4}$  M and a decarboxylation rate constant of 0.035 s<sup>-1</sup>. Comparison with ENH<sup>+</sup> reveals that the polymer has a considerably higher affinity for OA<sup>2-</sup>, but its adduct decarboxylates at an appreciably slower rate. It would appear from these observations that the dominant mode of binding does not involve the primary amine sites but possibly occurs at the quaternary amine sites.

Enamines were observed to be formed when, instead of OA<sup>2-</sup>, its esters were bound to the polymer, and this was cited as evidence that a Schiff-base mechanism is involved in decarboxylation.<sup>23</sup> Our results lend support to this conclusion because ENH<sup>+</sup> should be a good model for a polymer primary amine site and we have found 4-EtOA<sup>-</sup> to be a very sensitive spectral probe for Schiff-base formation. It should be emphasized once again that important quantitative differences exist between the behavior of 4-EtOA<sup>-</sup> and OA<sup>2-</sup> toward ENH<sup>+</sup>, and it is likely that these are carried over into the chemistry of the polymer.

Finally, it is of interest to compare divalent metal ion catalysis of OA<sup>2-</sup> decarboxylation with amine catalysis. Metal ion catalysis proceeds via the formation of M(OA)<sub>keto</sub><sup>13,28,29</sup> complexes, which are analogous to the imine adduct. Also, in a dead-end side reaction analogous to enamine formation, the metal complex forms an unreactive enol. The absolute rate constant for the decarboxylation of one of the most reactive complexes, Cu(OA<sub>keto</sub>), has been found by us to be 0.17 s<sup>-1</sup>,<sup>13</sup> a value almost two orders of magnitude lower than was found here for the protonated imine. Relatively fast decarboxylation rates are observed with the metal ions, however, because their OA<sup>2-</sup> complexes are more stable and are formed considerably more rapidly than the imines. Because of this, certain metal ions, e.g., Cu<sup>2+</sup> and Zn<sup>2+</sup>,<sup>14</sup> are almost as good catalysts as the amines.

**Acknowledgments.** We wish to express our appreciation to the National Science Foundation for its support of this work.

#### Appendix

The calculation of the three theoretical first-order relaxation rate constants for a given set of reaction conditions is described in this section. The subscript  $\Sigma$  refers to the summation over the concentrations of all the protonated and unprotonated forms of a given species.

The following independent rate equations apply to reaction Scheme I.

$$-d[\text{OA}]_{\Sigma}/dt = k_a[\text{ENH}^+][\text{OA}] - k_{-a}[\text{imine}]_{\Sigma} \quad (1a)$$

$$-d[\text{imine}]_{\Sigma}/dt = (k_{-a} + k_b + k_c)[\text{imine}]_{\Sigma} - k_a[\text{ENH}^+][\text{OA}] - k_{-b}[\text{enamine}]_{\Sigma} \quad (2a)$$

$$-d[\text{enamine}]_{\Sigma}/dt = k_{-b}[\text{enamine}]_{\Sigma} - k_b[\text{imine}]_{\Sigma} \quad (3a)$$

Casting these equations into differential form for the conditions  $[\text{EN}]_{\text{total}} \gg [\text{OA}]_{\text{total}}$  leads to the following relaxation matrix, the solutions of which for a given set of rate constants, pH, and  $[\text{EN}]_{\text{total}}$  are the three theoretical pseudo-first-order rate constants for the reaction system:

$$\begin{vmatrix} k_a[\text{ENH}^+] - \lambda & -k_{-a} & 0 \\ -k_a[\text{ENH}^+] & k_a + k_b + k_c - \lambda & -k_{-b} \\ 0 & -k_{-b} & k_{-b} - \lambda \end{vmatrix} = 0 \quad (4a)$$

(28) R. Steinberger and F. H. Westheimer, *J. Am. Chem. Soc.*, **73**, 429 (1951).

(29) E. Gelles and R. W. Hay, *J. Chem. Soc.*, 3673 (1958); E. Gelles and A. Salama, *ibid.*, 3684, 3689 (1958).

(26) E. J. Stamhuis, W. Maas, and H. Wynberg, *J. Org. Chem.*, **30**, 2160 (1965).

(27) M. Birus and D. L. Leussing, to be published.



The dependence of the rate constants in (4a) on  $[H^+]$  and the distribution of the specific species is derived as follows from the detailed reaction scheme given in Table III.

Let  $\alpha$  represent the fraction of the total amount of a species present in a given state of protonation. Then

$$\alpha_{\text{OA}} = 1/(1 + 10^{4.0}[H^+]) \quad (5a)$$

$$\alpha_{\text{HOA}} = 1 - \alpha_{\text{OA}} \quad (6a)$$

$$\alpha_{1,\text{imine}} = 1/(1 + K_4[H^+] + K_4K_5[H^+]^2) \quad (7a)$$

$$\alpha_{2,\text{imine}} = K_4[H^+]/(1 + K_4[H^+] + K_4K_5[H^+]^2) \quad (8a)$$

$$\alpha_{3,\text{imine}} = K_4K_5[H^+]^2/(1 + K_4[H^+] + K_4K_5[H^+]^2) \quad (9a)$$

$$\alpha_{1,\text{enamine}} = 1/(1 + K_6[H^+] + K_6K_7[H^+]^2) \quad (10a)$$

$$\alpha_{2,\text{enamine}} = K_6[H^+]/(1 + K_6[H^+] + K_6K_7[H^+]^2) \quad (11a)$$

$$\alpha_{3,\text{enamine}} = K_6K_7[H^+]^2/(1 + K_6[H^+] + K_6K_7[H^+]^2) \quad (12a)$$

The enamine/ketimine ratios of the di- and triprotonated adducts are functions of the ratio,  $R_1$ , for the monoprotionated adduct and the adduct protonation constants:

$$R_2 = (K_6/K_4)R_1 \quad (13a)$$

$$R_3 = (K_6K_7/K_4K_5)R_1 \quad (14a)$$

Applying the relationships defined by eq 5a-14a gives

$$k_a = (k_3 + k_4[H^+])\alpha_{\text{OA}} + k_5[H^+]\alpha_{\text{HOA}} \quad (15a)$$

$$k_{-a} = k_3/K_3\alpha_{\text{imine}} + k_4/(K_3K_4)\alpha_{2,\text{imine}} + k_5/(K_3K_4K_5)\alpha_{3,\text{imine}} \quad (16a)$$

$$k_b = k_6\alpha_{1,\text{imine}} + k_7\alpha_{2,\text{imine}} \quad (17a)$$

$$k_{-b} = (k_6/R_1)\alpha_{1,\text{enamine}} + (k_7/R_2)\alpha_{2,\text{enamine}} \quad (18a)$$

$$k_c = k_8 \quad (19a)$$

The three eigenvalues of (4a) are calculated from the following:

$$\lambda_{1,\text{calcd}} = 2(-P/3)^{1/2} \cos(\phi/3) \quad (20a)$$

$$\lambda_{2,\text{calcd}}, \lambda_{3,\text{calcd}} = 2(P/3)^{1/2} \cos(60^\circ \pm (\phi/3)) \quad (21a)$$

where

$$\phi = \tan^{-1}(\sqrt{-\Delta}/q\sqrt{27}) \quad (22a)$$

$$\Delta = 4P^3 + 27/q^2 \quad (23a)$$

$$P = b - a^2/3 \quad (24a)$$

$$q = c - ab/3 + 2a^3/27 \quad (25a)$$

$$a = -(k_a[\text{ENH}^+] + k_{-a} + k_b + k_c + k_{-b}) \quad (26a)$$

$$b = k_a(k_{-a} + k_{-b})[\text{ENH}^+] + k_{-b}(k_{-a} + k_c) + k_a(k_{-a} + k_b + k_c)[\text{ENH}^+] \quad (27a)$$

$$c = -k_a(k_{-a} + k_c)k_{-b}[\text{ENH}^+] - k_a k_{-a} k_{-b}[\text{ENH}^+] \quad (28a)$$

Owing to the excess of EN,  $[\text{ENH}^+]$  is easily calculated for a given experiment from the total EN, the  $\text{p}K_a$ s of EN and the given pH. The sum of the squares of the differences,  $\lambda_{3,\text{obsd}} - \lambda_{3,\text{calcd}}$  and  $\lambda_{2,\text{obsd}} - \lambda_{2,\text{calcd}}$ , are simultaneously minimized by varying the parameters defined in Table III.

For a detailed discussion of relaxation methods, ref 30 is recommended.

(30) Manfred Eigen and L. de Maeyer in "Techniques of Organic Chemistry", Vol. VIII, Part II, A. Weissberger, Ed., Wiley, New York, 1963.

## Formation and Reaction of Oxaziridine Intermediate in the Photochemical Reaction of 6-Cyanophenanthridine 5-Oxide at Low Temperature

Kunihiro Tokumura, Hitomi Goto, Hironobu Kashiwabara, Chikara Kaneko, and Michiya Itoh\*

Contribution from the Faculty of Pharmaceutical Sciences, Kanazawa University, Takara-machi, Kanazawa 920, Japan. Received January 4, 1980

**Abstract:** A stable oxaziridine intermediate in the photorearrangement reaction of 6-cyanophenanthridine 5-oxide was detected by matrix stabilization in ethanol and in 2-methyltetrahydrofuran (MTHF) solutions at 77 K. The oxaziridine intermediate trapped in these glassy solvents at 77 K affords 5-ethoxyphenanthridone and 6-cyanophenanthridine at the temperature allowing thermal reaction with solvent molecules, respectively. Remarkable excitation-wavelength dependence upon the formation of oxaziridine was observed at 77 K. Temperature dependences of the fluorescence quantum yield ( $\phi_f$ ) of the *N*-oxide and of the quantum yield ( $\phi_r$ ) of the formation of oxaziridine afford almost the same activation energies in these processes. This fact suggests that the formation of oxaziridine is competitive with the fluorescence decay of the lowest singlet excited state of the *N*-oxide. The photochemical reactions of the oxaziridine in ethanol glass and in MTHF glass at 77 K to form 6-cyano-3,1-dibenzoxazepine are also reported.

Since oxaziridine intermediates have been proposed in numerous investigations of the photorearrangement reactions of aromatic amine oxides,<sup>1</sup> some attempts to confirm this intermediate have been carried out by laser flash photolysis. Lohse<sup>2</sup> reported very rapid formation of isoquinolone within the duration of a ruby laser pulse in the photorearrangement reaction of isoquinoline 2-oxide. He suggested that the reaction cannot include such an intermediate as an oxaziridine. Further, Tomer et al.<sup>3</sup> also reported a mech-

anism without the formation of a transient oxaziridine in the photorearrangement of 3,6-diphenylpyridazine 1-oxide by ruby laser spectroscopy. On the other hand, some attempts to detect an unstable intermediate in the photorearrangement reaction at low temperature have been reported. Jerina et al.<sup>4</sup> reported oxygen walks and keto tautomers of phenol in the photolysis of arene oxide at low temperature.

Recently, Kaneko et al.<sup>5</sup> reported that the photolysis of 6-cyanophenanthridine 5-oxide (**I**) in ethanol at room temperature

(1) (a) C. Kaneko, *J. Synth. Org. Chem. Jpn.*, **26**, 758 (1968); (b) G. G. Spence, E. C. Taylor, and O. Buchardt, *Chem. Rev.*, **70**, 231 (1970); (c) F. Bellamy and J. Streith, *Heterocycles*, **4**, 1391 (1976).

(2) C. Lohse, *J. Chem. Soc., Perkin Trans 2*, 229 (1972).

(3) K. B. Tomer, N. Harrit, I. Rosenthal, O. Buchardt, K. L. Kumler, and D. Creed, *J. Am. Chem. Soc.*, **95**, 7402 (1973).

(4) D. M. Jerina, B. Witkop, C. L. McIntosh, and O. L. Chapman, *J. Am. Chem. Soc.*, **96**, 5578 (1974).

(5) C. Kaneko, R. Hayashi (nee Kitamura), M. Yamamori, K. Tokumura, and M. Itoh, *Chem. Pharm. Bull.*, **26**, 2508 (1978).